REMARKS

In the office action, the examiner rejected Claims 16, 21-23 and 40 under 35 U.S.C. 112, first paragraph, as failing to comply with the written description requirement. It is stated that, in Claims 16 and 40, the feature "wherein, in the drilling operation, when hardness H of the workpiece W is lower than 500 [Hv], a peripheral velocity V of the drill D is higher than (175 - H / 4) [m/min] and a feed amount of the drill per one revolution is smaller than 0.03 mm" is not described in the instant specification. Further, it is stated that, in Claims 16 and 40, the feature "when the hardness H of the workpiece W is higher than 500 [Hv], the peripheral velocity V of the drill D is higher than 50 [m/min] and the feed amount of the drill D per one revolution is smaller than 0.03 mm" is not described in the instant specification.

In the previous amendment of Claim 16 and in new Claim 40, the applicant has inadvertently recited that "the feed amount of the drill D per one revolution is smaller than 0.03 mm" where the value "0.03 mm" should be --0.3 mm-- as described in the paragraph [0071] in the specification. Accordingly, the applicant has amended Claims 16 and 40 concurrently herewith to correct the numerical value to --0.3 mm--. Please note that this amendment is to correct the obvious error in the claims and thus not to cause a new issue problem to the pending claims. Therefore, even though this office action is final, the applicant respectfully requests the examiner

that the foregoing amendment be entered without raising the new issue problem.

In the office action, the examiner rejected Claims 16, 21-23 and 40 under 35 U.S.C. 103(a) as being unpatentable over Blechner (U.S. Patent No. 3,117,042). In the response to the previous office action, the applicant has added the limitations to Claim 16 and 40 to more clearly differentiate the present invention from the technologies disclosed by the prior art.

More specifically, the applicant has added the limitations to Claim 16 so that the features of the present invention reside in that (1) the drilling operation on a machined surface of the workpiece to impart a large local strain to the machined surface, (2) drilling operation causes the machined surface of the workpiece to be subjected to a plastic working with a true strain of at least 1, such that said ultrafine crystal layer is formed on the machined surface, (3) in the drilling operation, when hardness H of the workpiece W is lower than 500 [Hv], a peripheral velocity V of the drill D is higher than (175 - H / 4) [m/min] and a feed amount of the drill per one revolution is smaller than 0.3 mm, and when the hardness H of the workpiece W is higher than 500 [Hv], the peripheral velocity V of the drill D is higher than 50 [m/min] and the feed amount of the drill D per one revolution is smaller than 0.3 mm, and (4) the drilling operation is performed for the workpiece made of steel material with a material temperature at the machined surface being held in a range which is higher than an Ac1

transformation point of the steel material and lower than a melting point of the steel material.

It should be noted that, in the present invention, it is essential that, when the workpiece is constituted by a metallic material, (a) the drilling operation on a machined surface of the workpiece is conducted under the condition noted in the feature (4) in combination with (b) to impart a large local strain to the machined surface, (2) drilling operation is conducted by the condition defined in the feature (3). Only when such a combination is established, the machined surface of the workpiece is subjected to a plastic working with a true strain of at least 1, thereby forming the ultrafine crystal layer on the machined surface. This effect is exemplified by, for example, an article "A microstructural investigation of the surface of a drilled hole in carbon steel", J.G. Li, M. Umemoto, Y Todaka, K. Tsuchiya, Acta Materialia, 2006, a copy of which is attached as a reference.

The features of the present invention defined in Claim 40 are the same with respect to the features (1)-(3) of Claim 16 noted above. Instead of the feature of Claim 16 noted above, the present invention defined in Claim 40 includes the feature (5) that the drilling operation is performed on the surface of the workpiece made of a non-steel material with a material temperature at the machined surface being held in a range which is higher than substantially half a melting point of the non-steel material and is lower than the melting point of the non-steel material.

Again, it should be noted that, in the present invention, it is essential that, when the workpiece is constituted by a non-steel metallic material, (a) the drilling operation on a machined surface of the workpiece is conducted under the condition noted in the feature (5) in combination with (b) to impart a large local strain to the machined surface, (2) drilling operation is conducted by the condition defined in the feature (3). Only when such a combination is established, the machined surface of the workpiece is subjected to a plastic working with a true strain of at least 1, thereby forming the ultrafine crystal layer on the machined surface.

The cited Blechner reference is directed to the heat-treatment of metals for hardening. As recited in Claims 16 and 40, the present invention is directed to the drilling operation to improve the hardness, etc., of the machined surface of the workpiece. Rather than the drilling operation, the Blechner reference shows the pressing operation by a machine tool, which is mechanically different from the drilling operation and is not able to form an ultrafine crystal layer even when exerting the true strain greater than 1 under the temperature condition identical to the present invention. Especially, the present invention includes the feature (3) noted above which specifically define the relationship among the hardness of the workpiece and the peripheral velocity and feed amount of the drill. This feature is not shown or suggested by the cited Blechner reference. Thus, the present invention is not obvious over the cited Blechner reference.

In view of the foregoing, the applicant believes that the instant application is in condition for allowance, and accordingly, the applicant respectfully requests that the present application be allowed and passed to issue.

Respectfully submitted,

MURAMATSU & ASSOCIATES

Dated: 10/11/2010

By: _____

Yasuo Muramatsu
Registration No. 38,684
Attorney of Record
114 Pacifica, Suite 310
Irvine, CA 92618
tel: (949) 753-1127

AMD-KN14.005
100810

Available online at www.sciencedirect.com
ScienceDirect
Acta Materialia 55 (2007) 1397–1406
Acta MATERIALIA
www.actamat-journals.com

# A microstructural investigation of the surface of a drilled hole in carbon steels

J.G. Li [a,b,*], M. Umemoto [a], Y. Todaka [a], K. Tsuchiya [a]

[a] *Department of Production Systems Engineering, Toyohashi University of Technology, Toyohashi, Aichi 440-0038, Japan*
[b] *Department of Superalloy, Institute of Metal Research, Chinese Academy of Sciences, No. 72, Wenhua Road, Shenyang 110016, PR China*

Received 30 August 2006; received in revised form 26 September 2006; accepted 26 September 2006
Available online 13 December 2006

**Abstract**

The microstructure of the surface of drilled holes generated under different drilling conditions in carbon steels has been investigated. It is found that the surface microstructure depends strongly on the drilling parameters and the hardness of the matrix. White etching layers, composed of an equiaxed nanocrystalline structure layer with an average grain size of the order of several 10 nm and a submicron grained layer containing fresh martensite along the depth, formed on the hole surfaces during drilling at moderate to high cutting speed in carbon steels with high matrix hardness. The existence of a high content of austenite at the hole surface suggests that dynamic phase transformation (DPT) from body-centered cubic to face-centered cubic occurred during high-speed drilling. It is proposed that the ultra-fine structure layer on the surface of a drilled hole is produced by severe plastic deformation-induced DPT together with a large strain gradient and high strain rate.


*Keywords:* Nanocrystalline structure; Dynamic phase transformation; Severe plastic deformation; Drilling; Carbon steels

## 1. Introduction

Drilling has been widely used in manufacturing as a process to remove material. It has been reported that drilling accounts for nearly 40% of all the metal removal operations in the aerospace and automobile industries [1]. During drilling, metallurgical transformation and, perhaps, chemical interactions take place near the hole surface in workpieces due to the intense, localized and rapid thermal mechanical working. Thus the worked surface can show an extremely different structure from the bulk material. This type of problem has attracted substantial research in the field of so-called "surface integrity", a term encompassing all aspects of surfaces, such as residual stress, microhardness, surface finish and microstructure [2]. It is believed that the surface integrity has a strong impact on the performance of a product. The conventional manufacturing process consists of matrix drilling in the soft state, followed by hardening using heat treatment [3]. The influence of the surface integrity, such as microstructure and residual stress, introduced by drilling is thereby decreased or removed completely. Recently, with increasing demands on dimension accuracy and higher production rates, the high-speed drilling of hardened materials as a finishing process has become applicable due to the development of tough tools with high abrasion resistance. As a finishing process, the surface microstructures introduced by the drilling remain in the final products. Therefore, to guarantee the mechanical properties of components, the surface microstructure of the drilled parts becomes progressively more important. Field et al. [4] and Griffith [5] studied the microstructure adjacent to drilled holes in hardened steels and reported that a so-called white etching layer (WEL) formed on the hole surface. The term WEL originated from the fact that it appears white under the optical microscope. In the literature, WELs have been widely reported in many material

* Corresponding author. Tel.: +81 532 47 0111x5218; fax: +81 532 44 6690.
*E-mail address:* lijinguo@martens.pse.tut.ac.jp (J.G. Li).

1359-6454/$30.00 
doi:10.1016/j.actamat.2006.09.043

removal processes, such as turning [6,7], grinding [8,9], electrical discharge machining (EDM) [10] and milling [11], as well as drilling [4,5]. However, the formation mechanisms and microstructure of WEL produced in machining of hardened steels are still not clearly understood. It is commonly thought that the WEL is composed of untempered martensite ($\alpha$) and austenite ($\gamma$). The volume fractions of $\alpha$ and $\gamma$ in the WEL have been a controversial subject discussed in a number of papers. Tönshoff [12] and Chou and Evans [6] have reported that the volume fraction of retained austenite in WEL increases threefold compared with that in virgin work material with 11%. In contrast, Akcan et al. [13] suggest that the amount of $\gamma$, if any, is much less than 10% in the WEL after turning the same material used in Refs. [6,12]. Remash et al. [14] reported that the volume fraction of $\gamma$ in the WEL is changed with the cutting speed. Two different proposals on the formation mechanism of the WEL have been proposed, corresponding to the different compositions of the WEL. One is that the deformation of material due to very large strain is the principal factor contributing to the formation of the WEL with a low $\gamma$ content [14,15]. The other is that the WEL is a phase-transformed layer where re-austenization occurs during machining due to rapid heating and cooling combined with the high pressure generated by the action of the tool [6,12]. Furthermore, the effect of the white layer on component performance has still not been clarified and is not well understood. Some researchers consider that the WEL is detrimental to the fatigue properties of the component [4,16], while others have reported that the WEL is beneficial to tribology [16–18]. It has also been suggested that the fatigue strength depends on the machining process [19]. Therefore, to clarify the aforementioned controversial subjects and to optimize the performance of the machined surface, more experiments are needed if today's industrial production and scientific research are to understand and characterize the surface microstructure produced by the different machining processes and process parameters.

In the present study, the microstructures near the surface of holes drilled under different conditions in carbon steels with different matrix structures are investigated by detailed characterization involving scanning electron microscopy (SEM), transmission electron microscopy (TEM), X-ray diffraction (XRD) and the Vickers microhardness tester. It is found that the surface microstructure depends strongly on the drilling parameters and the matrix hardness. The WEL is observed on hole surfaces drilled at a moderate to high cutting speed when the matrix hardness is above a certain value. The formation mechanism of the WEL on the drilled hole surface is discussed based on the microstructural observation and XRD analysis.

## 2. Experimental procedures

The materials used in this study were Fe–0.56% C steels in ferrite and pearlite, martensite and tempered martensite structures; Fe–0.80% C steels in martensite, fine lamellar pearlite and coarse lamellar pearlite structures; and a commercial bearing steel (SUJ2) in a tempered martensite structure. The nominal chemical compositions of the steels are given in Table 1. For Fe–0.56% C and Fe–0.80% C steels, martensite structures were prepared by austentizing at 1273 K for 3.6 ks and then quenching in ice water. Coarse and fine pearlite structures were obtained by isothermal transformations at 963 and 893 K, and the interlamellar spacings of coarse and fine pearlite were about 900 and 170 nm, respectively. For SUJ2 steel, the specimen was annealed at 1103 K for 30 min, oil quenched at 323 K and then tempered at 443 K for 40 min. The drilling experiments were performed at cutting speeds from 20 to 100 m/min with feeding rate from 0.01 to 0.05 mm/rev by using a sintered carbide drill with diameters of 2.5 and 5.0 mm. Oil mist was used as a coolant. The microstructure was characterized using SEM, TEM and XRD. SEM observations were carried out on a JEOL JSM-6500FT microscope after polishing and etching the samples with 5% Nital. TEM observations were performed on a Hitachi H-800 transmission electron microscope working at 200 kV. XRD analysis was conducted on a RINT-2500VHF X-ray diffractometer with Cu K$\alpha$ radiation. Quantitative phase analysis was carried out using Rietveld software QUANTO. The hardness measurement was carried out using a MVK-G1Vickers microhardness tester with a load of 98 mN holding for 10 s.

## 3. Results and discussions

### 3.1. The microstructures near the hole surface

#### 3.1.1. The influence of the matrix microstructure

To check the influence of the matrix structure on the hole surface, the microstructures near the hole surface drilled at a cutting speed of 80 m/min with feed rate of 0.05 mm/min in Fe–0.56% C and Fe–0.80% C steels were observed by SEM and TEM. Fig. 1 shows the typical cross-sectional (section perpendicular to hole axis) SEM micrographs near the hole surface in Fe–0.56% C steels with different matrix microstructures. The Vickers microhardness values of different matrix structures are presented in the images. When the matrix structure is pearlite with a lower hardness of 2.9 GPa (Fig. 1a), only a heavily flowed microstructure is seen at the top surface. For the tempered martensite specimen with a hardness of 4.5 GPa, WELs with a thickness of about 4.5 μm are observed (Fig. 1b). For the as-quenched martensite specimen with a hardness

Table 1
The nominal chemical composition of the used carbon steels (figures in wt.%)

| | C | Si | Mn | P | S | Cr | Fe |
|---|---|---|---|---|---|---|---|
| Fe–0.56% C | 0.56 | 0.20 | 0.72 | 0.12 | 0.014 | 0.10 | Balance |
| Fe–0.80% C | 0.80 | 0.20 | 1.33 | 0.010 | 0.0003 | – | Balance |
| SUJ2 | 1.10 | 0.35 | 0.50 | 0.025 | 0.025 | 1.60 | Balance |

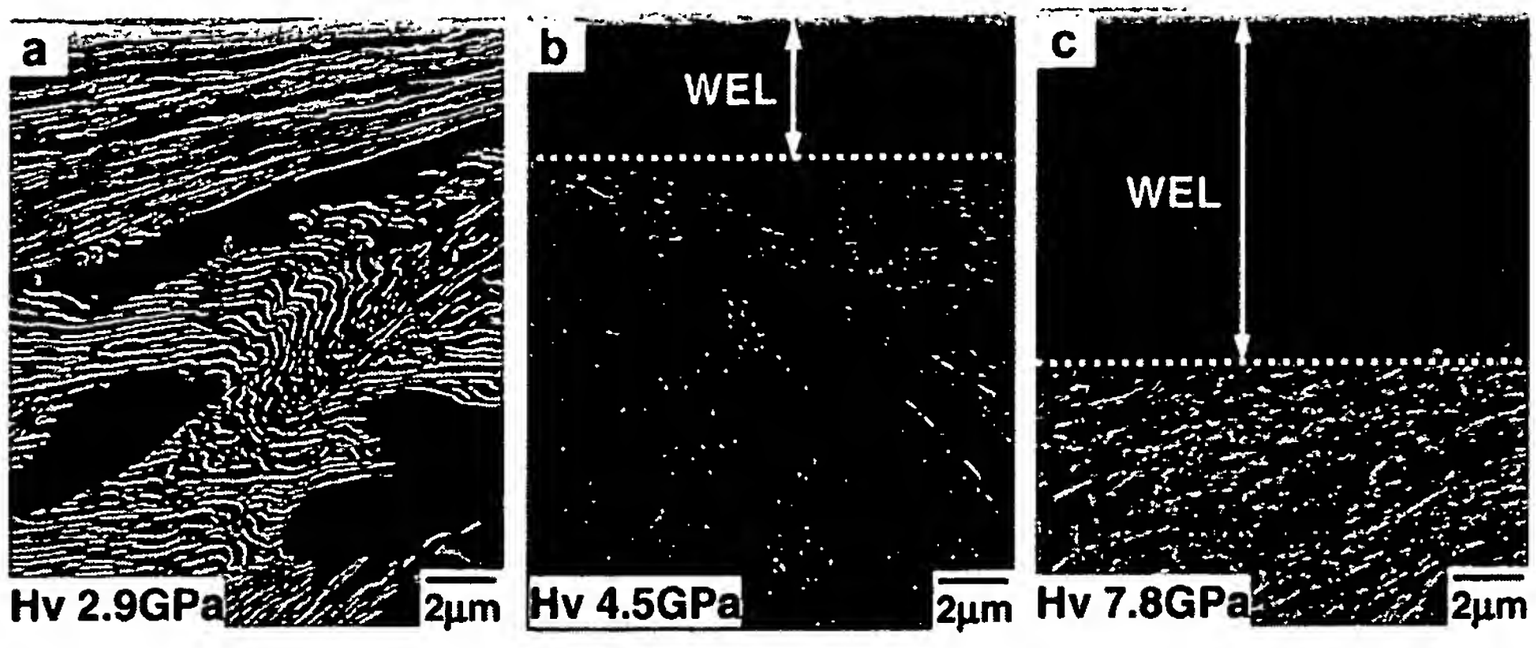


Fig. 1. Cross-sectional (section perpendicular to hole axis) SEM micrographs near the hole surface in Fe–0.56% C steels with different matrix microstructures (cutting speed: 80 m/min, feeding rate: 0.05 mm/rev, drill diameter: 5.0 mm). (a) Pearlite, (b) tempered martensite and (c) martensite. The Vickers microhardness values of different matrix structures are shown in the images.

of 7.8 GPa, a WEL with a thickness of about 11 μm is generated on the hole surface (Fig. 1c). In each case, beneath the WEL, the deformed flow structure, which is inclined to the cutting direction, can be seen, which indicates that severe deformation occurred near the drilled hole surface.

Fig. 2 shows typical cross-sectional SEM micrographs near the hole surface in Fe–0.80% C steel with different matrix microstructures. The Vickers microhardness values of the different matrix structures are shown in the images. It is found that a WEL formed on the hole surface of all three structures. For the coarse lamellar pearlite of hardness 3.2 GPa, the thickness of the WEL is only around 1.0 μm (Fig. 2a). Although the fine lamellar pearlite is just a little harder than the coarse lamellar pearlite, the thickness of the WEL is increased to 3.0 μm, which is three times that of the coarse lamellar pearlite. When the matrix structure is as-quenched martensite with a hardness of 8.1 GPa, the thickness of the WEL is about 13.6 μm. Between the WEL and the matrix is a deformed layer. The correlation between the thickness of the WEL and the matrix hardness of the drilled Fe–0.56% C and Fe–0.80% C specimens obtained in the present study is plotted in Fig. 3. It is clear that the thickness of the WEL depends strongly on the matrix hardness, increasing in a roughly linear fashion with the matrix hardness.

Fig. 4a shows cross-sectional high-magnification SEM micrographs near the hole surface and a TEM image on the topmost surface of a drilled hole in Fe–0.56% C steel with a ferrite and pearlite microstructure. It is seen that the cementite plates become thinner and the interspacing of the cementite plates reduces close to the surface. On the topmost surface, all the cementite plates are orientated parallel to the cutting direction. Near the hole surface, various deformations of the cementite, such as bending, necking and fragmentation, are observed.

The microstructure on the topmost surface of the drilled holes was observed by TEM. The deformed structure with a high density of dislocation is observed, as show in Fig. 4b. The selected area diffraction (SAD) pattern indicates that the microstructure is composed of body-centered cubic (bcc) ferrite and cementite. Fig. 4c shows a dark field TEM micrograph taken from the first ring ($\{110\}_\alpha$) of

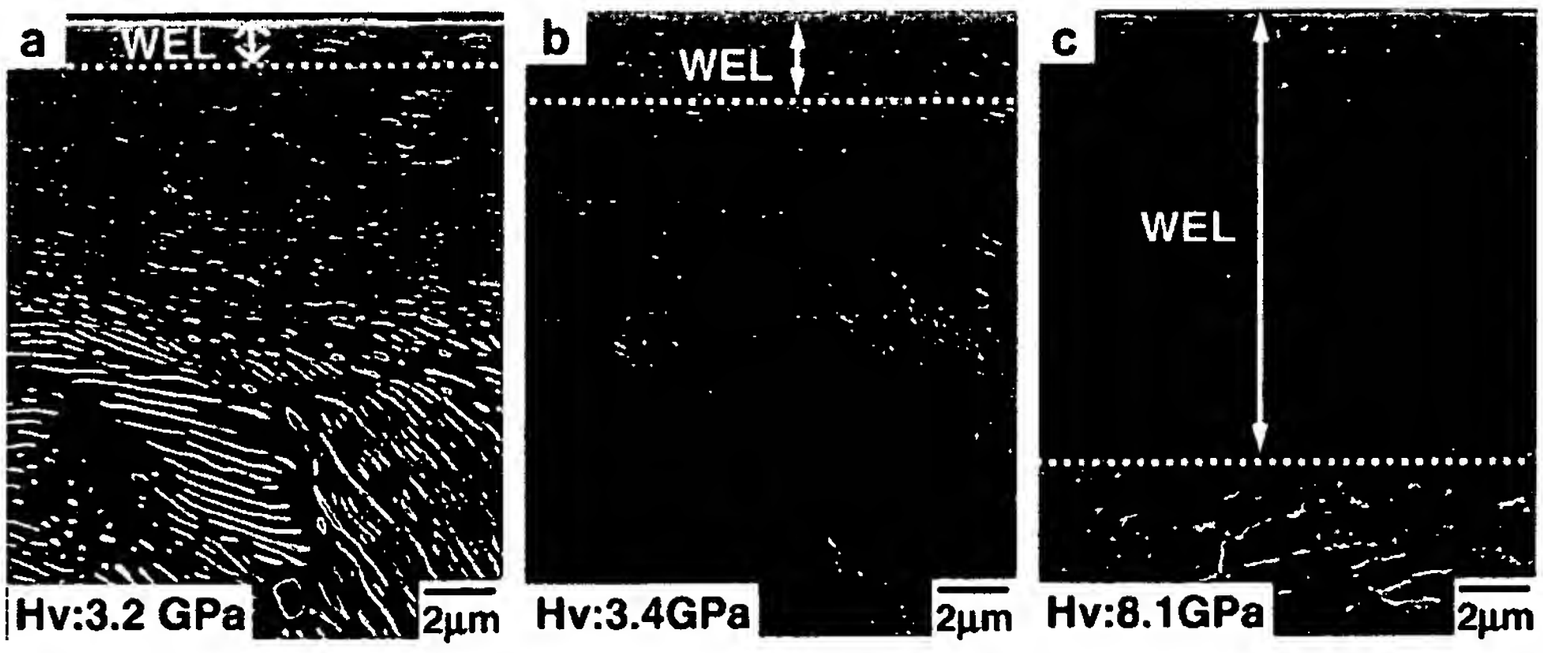


Fig. 2. Cross-sectional (section perpendicular to hole axis) SEM micrographs near the hole surface in Fe–0.56% C steels with different matrix microstructures (cutting speed: 80 m/min, feeding rate: 0.05 mm/rev, drill diameter: 5.0 mm). (a) Coarse lamellar pearlite, (b) fine lamellar pearlite and (c) martensite. The Vickers microhardness values of different matrix structures are shown in the images.

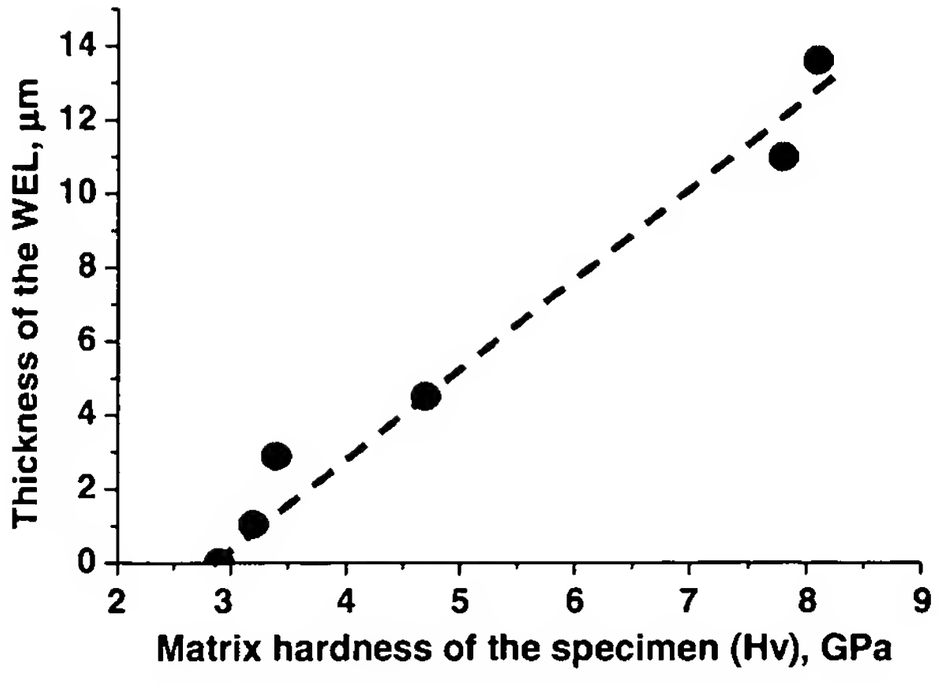


Fig. 3. Relationship between the thickness of WEL and matrix hardness of the specimen in carbon steels (cutting speed: 80 m/min, feeding rate: 0.05 mm/rev, drill diameter: 5.0 mm). The dash line is fitted according to the discrete experimental results.

SAD pattern in Fig. 4b. The grains are of irregular shape and several hundred nanometers in size, and some nanocrytalline cementite particles are seen. These results suggest that strong deformation occurred near the surface of the drilled hole.

Fig. 5 shows the cross-sectional SEM and TEM micrographs near the hole surface with high magnification in Fe–0.56% C steel with as-quenched martensite structure. The WEL has a sharp boundary with the adjacent microstructure on the surface of the drilled hole. It is noticed that the microstructure of the WEL is inhomogeneous with distance from the surface. Close to the topmost surface, a 2- to 3-μm-thick featureless microstructure layer is observed. TEM observation (Fig. 5b) shows that the microstructure of this layer consists of equiaxed grains with an average grain size of the order of 10 nm. The continuous rings of the SAD pattern indicate the polycrystalline nature of the material and the random orientation of the grains. This diffraction pattern is dominated by the strong diffraction rings from the bcc ferrite structure. It is noted that several diffraction rings can be interpreted as austenite reflections. Beneath the nanocrystalline structure layer, a submicron grain layer with a mixed structure of nano- to submicron-sized grains and grains with a twinned structure in the 100–200 nm size range (marked by the circles in Fig. 5c) is observed. Such a twinned structure is typical of high carbon steel martensite. The SAD pattern shows that the microstructure can be indexed as austenite, twinning martensite and ferrite. Due to the proximity of ferritic diffraction rings to the martensitic ones, the diffraction rings of ferrite are not given in Fig. 5c. Since the starting structure is lath martensite, it is considered that the twinned martensite is formed during quenching after drilling. Close to the bottom of WEL, submicron-sized deeply etched islands surrounded by a smooth contrast area are seen. From the similar etched contrast of islands with the ferrite just beneath the WEL, it was deduced that the island areas are retained ferrite (not re-austenization) and the surrounding smooth contrast areas are fresh martensite formed during quenching after drilling. These observed microstructures suggested that a re-austenite phase transformation occurred during drilling. Just below the WEL, a layer consisting of elongated ferrite grains with

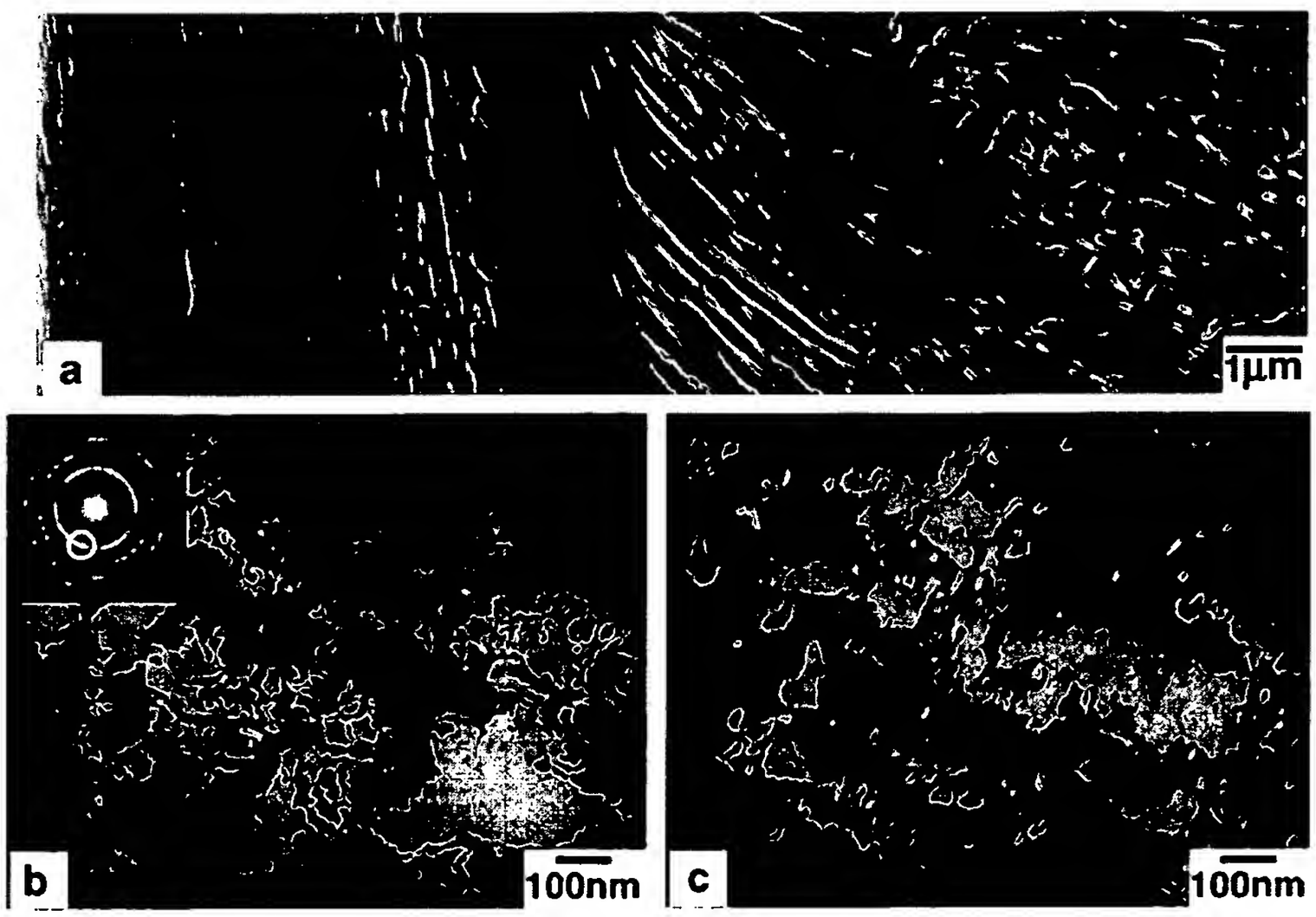


Fig. 4. Micrograph near surface of a hole in quenched Fe–0.56% C steel with a pearlite structure after drilling (cutting speed: 80 m/min, feeding rate: 0.05 mm/rev, drill diameter: 5.0 mm). (a) SEM image, (b) TEM bright field image and corresponding SAD pattern and (c) TEM dark field image taken from the first ring of SAD pattern marked in (b).

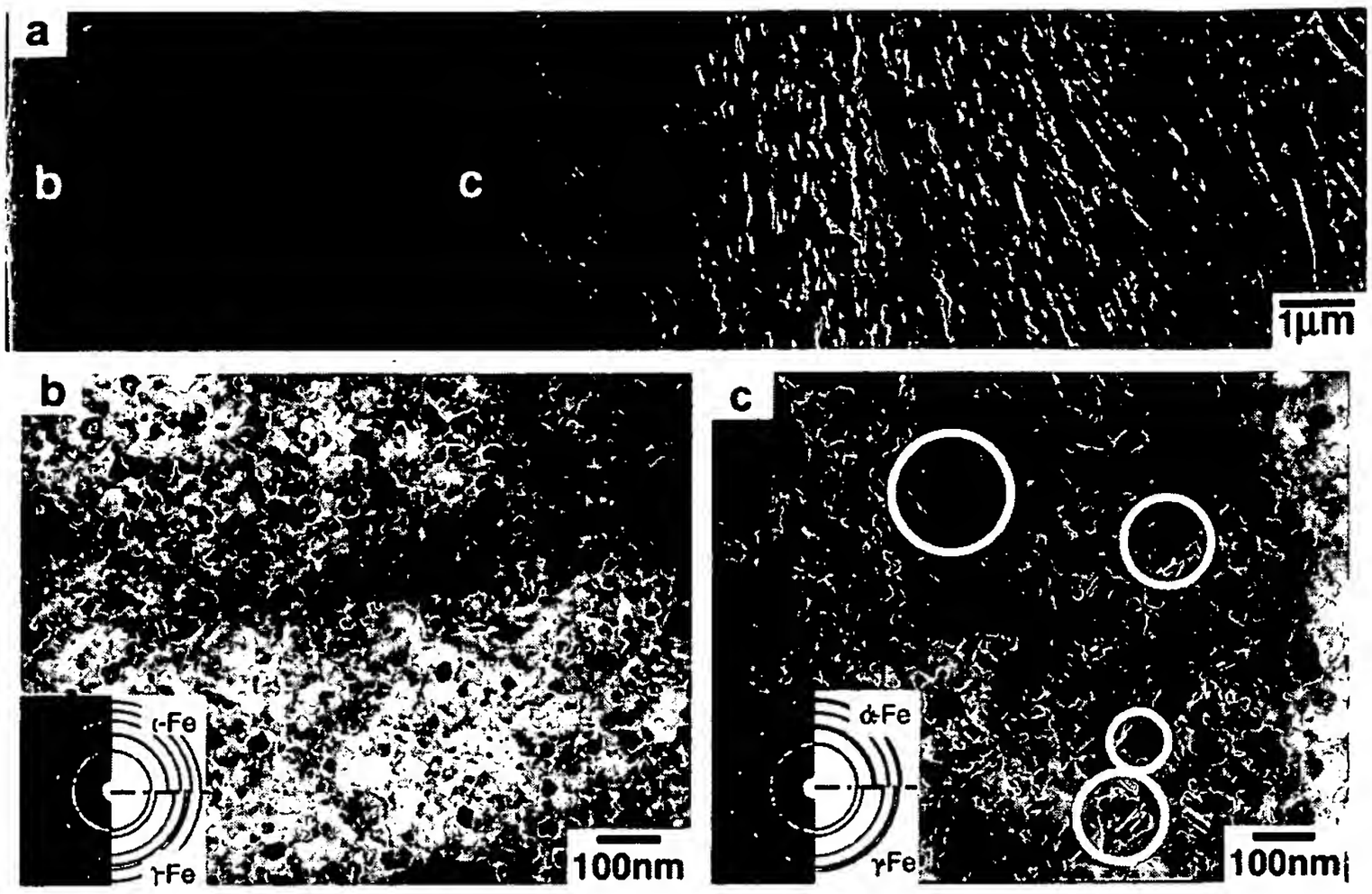


Fig. 5. Micrograph near surface of a hole in quenched Fe–0.56% C steel with a martensite structure after drilling (cutting speed: 80 m/min, feeding rate: 0.05 mm/rev, drill diameter: 5.0 mm). (a) SEM image and (b) and (c) TEM bright field images and corresponding SAD patterns of (b) and (c) marked in (a).

rod-shaped cementite particles precipitated at the grain boundaries are observed. This microstructure indicates that in this layer dynamic recrystallization occurred in the ferrite condition during high-speed drilling. The precipitated cementite particles suggest that the evident temperature rise occurred in this area during drilling. Between the recrystallized layer and matrix, a slightly tempered deformed martenstite structure layer is seen. In the literature, the recrystallized layer and deformed martensite structure layer are commonly referred to as 'dark layers' because of their dark appearance after etching under an optical microscope.

According to the above results, two layers – a nanocrystalline structure layer and a layer containing the submicron-sized twinned martensite and ferrite grains – can be identified in the WEL. Similar to the thickness of the WEL, the thickness of the nanocrystalline structure layer is also correlated to the matrix hardness, as shown in Fig. 6. It is seen that the thickness of the nanocrystalline structure layer increases roughly linearly with increasing matrix hardness when the drilling parameters are kept constant.

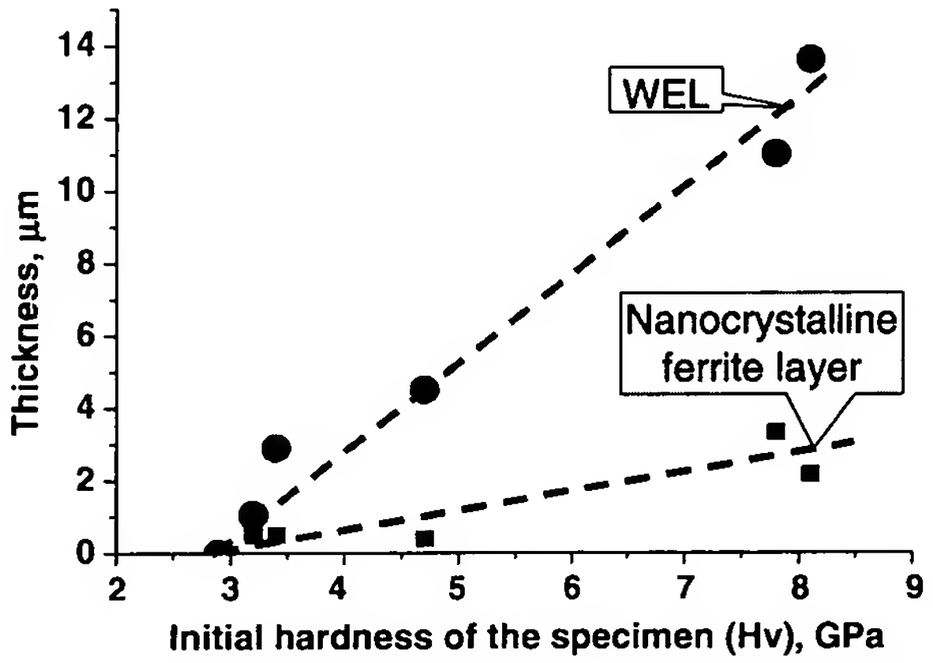


Fig. 6. Relationship of the thickness of the WEL, the nanocrystalline layer and the matrix hardness of the specimen in carbon steels (cutting speed: 80 m/min, feeding rate: 0.05 mm/rev, drill diameter: 5.0 mm). The dash lines are fitted according to the discrete experimental results.

*3.1.2. The influence of the drilling parameters*

The influence of the drilling parameters, such as cutting speed, feed rate and drill diameter, on the surface microstructure of a drilled hole is studied in Fe–0.56% C steel with an as-quenched martensite structure. Fig. 7 shows the effect of feed rate on the surface microstructure where the cutting speed and drilling diameter were kept constant. The thickness of the WEL is found to increase from 7.5 to 13 μm when the feed rate is enhanced from 0.01 to 0.10 mm/rev. Fig. 8 shows longitudinal section (section parallel to hole axis) SEM micrographs of the hole surface in Fe–0.56% C steel drilled at different cutting speeds keeping the feed rate and drilling diameter as constant. The surface microstructure of the drilled hole depends strongly on the cutting speed. For the low cutting speed of 20 m/min (Fig. 8a), only a deformed structure layer is seen at the top surface. However, the WELs are observed on the hole surface drilled with a moderate to high cutting speed. The thickness of the WEL increases from 8 to 15 cm when the cutting speed is changed from 60 to 100 m/min, as shown in Fig. 8b–d. The effect of the drill diameter on the surface microstructure was studied by drilling with a cutting speed of 80 m/min and a feed rate of 0.05 mm/rev. The thickness

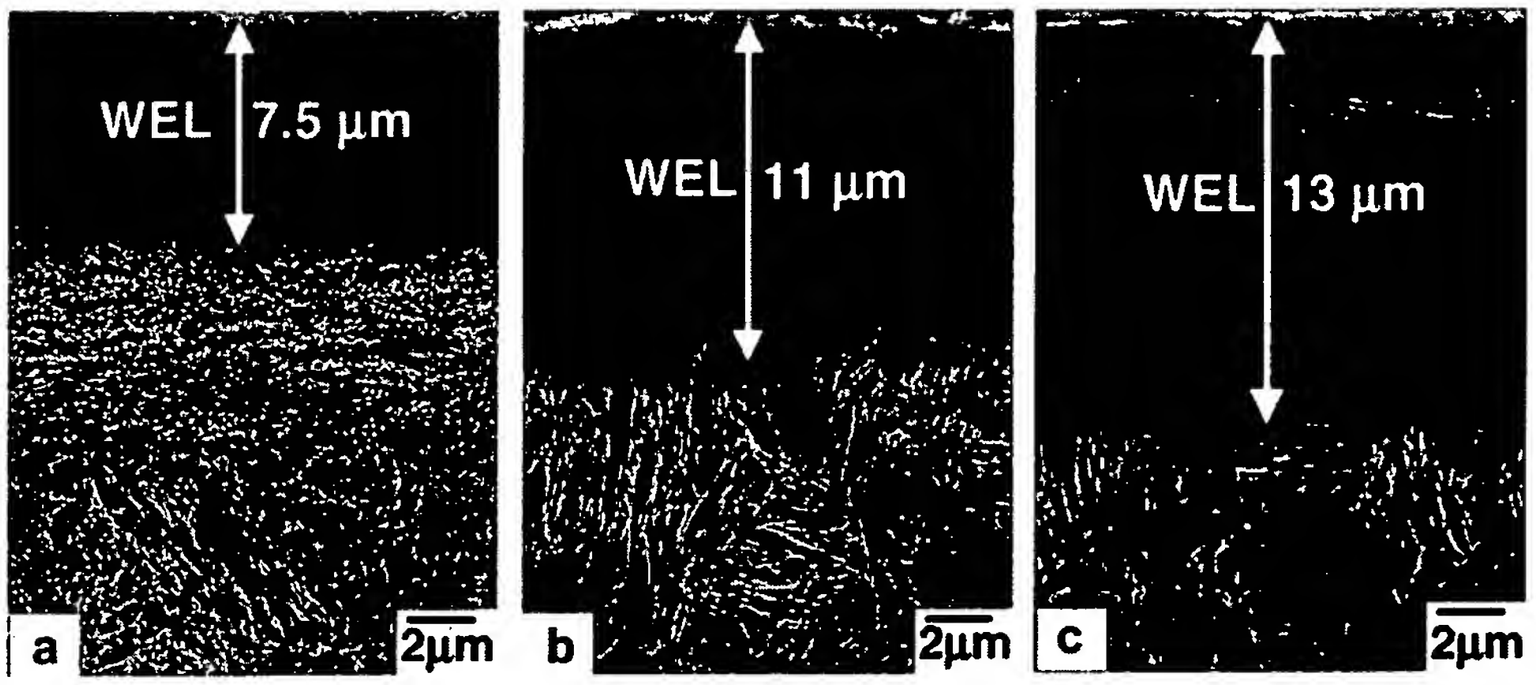


Fig. 7. SEM micrographs near the hole surface after drilling at different feed rates (cutting rate: 80 m/min, drill diameter: 5.0 mm). (a) 0.01 mm/rev, (b) 0.05 mm/rev and (c) 100 mm/rev.

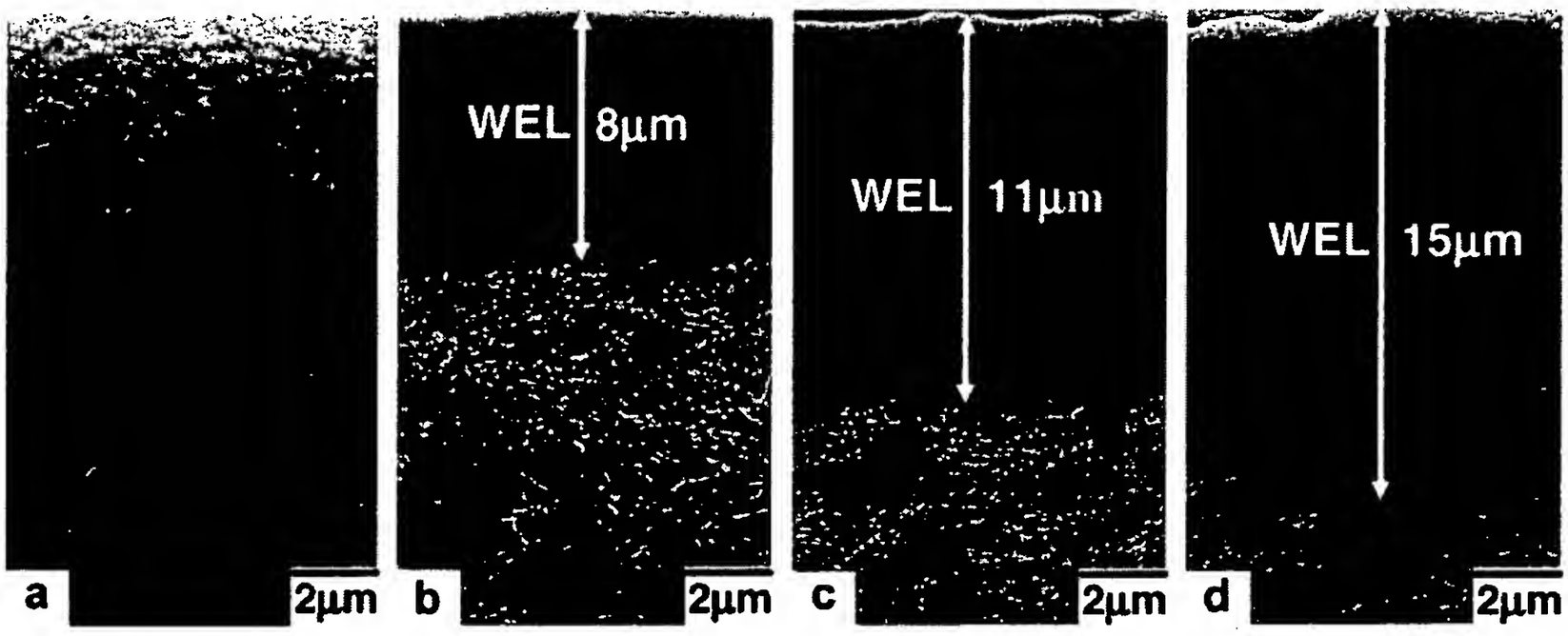


Fig. 8. SEM micrographs near the hole surface after drilling at different cutting speeds (feed rate: 0.05 mm/rev, drill diameter: 5.0 mm). (a) 20 m/min, (b) 60 m/min, (c) 80 m/min and (d) 100 m/min.

of WEL increases from 5.5 to 11 μm when the drill diameter is increased from 2.5 to 5.0 mm, as shown in Fig. 9a and b.

The influence of the drilling parameters on the surface microstructure of drilled hole has been also studied in SUJ2 steel with a tempered martensite structure. Fig. 10 shows the correlation between the thickness of the WEL and the drilling parameters. It is seen that the thickness of the WEL depends strongly on the drilling parameters. In the current drilling conditions, the WEL cannot be observed on the surface of the drilled hole until the cutting speed is more than 40 m/min. Similar to that of Fe–0.56% C steel, the thickness of the WEL increases with the enhancement of cutting speed and feed rate.

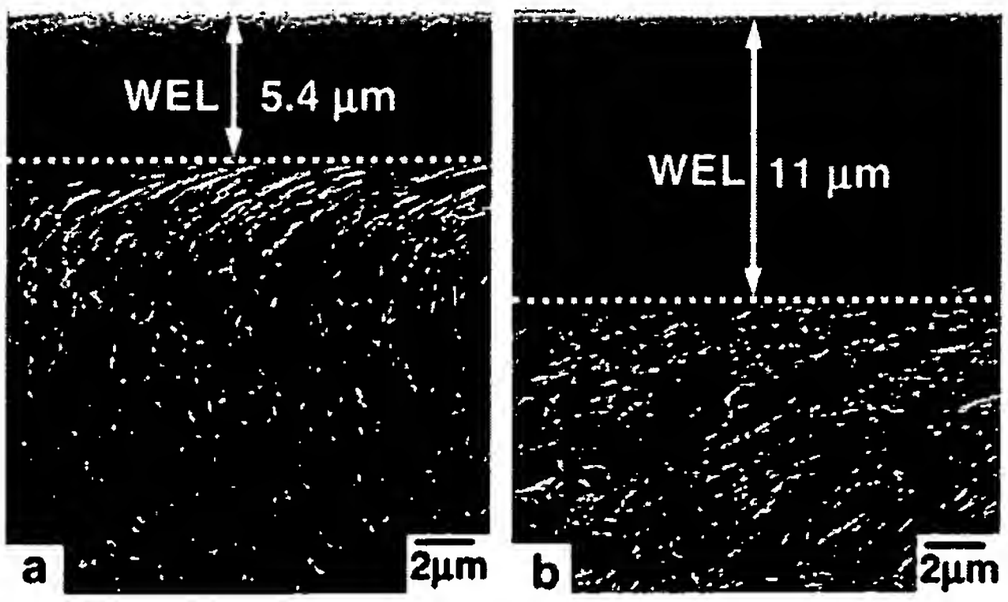


Fig. 9. SEM micrographs near the hole surface after drilling with different drill diameters (cutting rate: 80 m/min, feed rate: 0.05 mm/rev). (a) 2.5 mm and (b) 5 mm.

### 3.2. XRD spectra of the drilled hole surface

The phases which appear on the drilled hole surfaces in Fe–0.56% C and Fe–0.80% C steels were analyzed using XRD spectrometry. Fig. 11 shows the XRD spectra taken from matrix material of as-quenched martensite and drilled specimens of Fe–0.56% C steels. The XRD pattern of the matrix exhibits high-intensity α′-phase (martensite) peaks and very low-intensity retained austenite peaks. The quantitative analysis by XRD shows that the volume fraction of the retained austenite is less than 1%. In the XRD spectrum

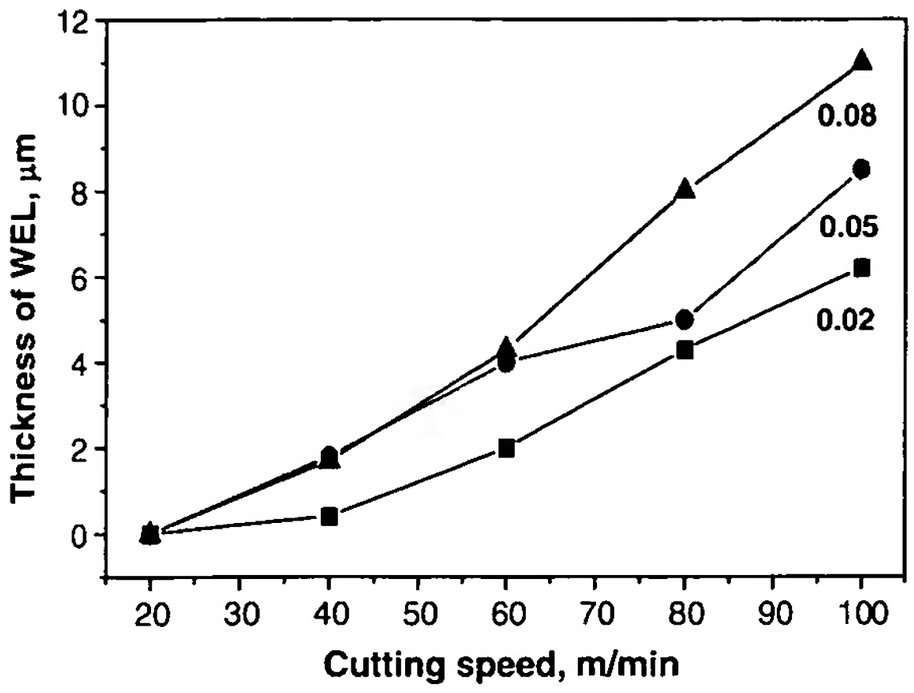


Fig. 10. The variation of the thickness of WELs with the cutting speed and feed rate after drilling in SUJ2 steel with a drill diameter of 2.5 mm. The numbers in the figure are the feed rate values.

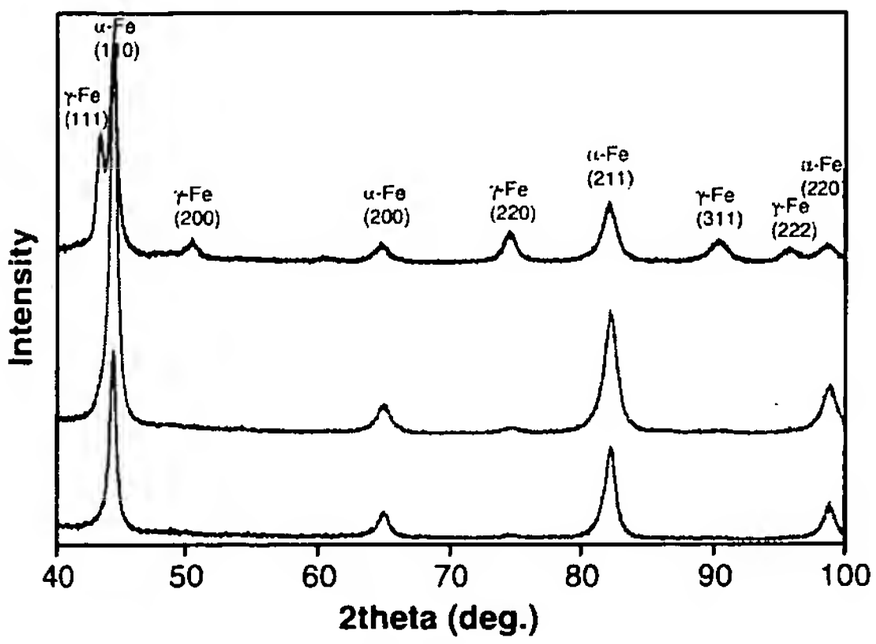


Fig. 11. X-ray diffraction spectra of quenched Fe–0.56% C with a martensite structure before and after drilling (cutting speed: 80 m/min, feeding rate: 0.05 mm/rev, drill diameter: 5.0 mm).

of the surface of a hole drilled at a cutting speed of 80 m/min with a feed rate of 0.05 mm/rev, the volume fraction of austenite is about 15%, which is substantially higher in comparison with that of the matrix. The XRD spectra of the hole surface in Fe–0.80% C steels drilled at a cutting speed of 80 m/min with a feed rate of 0.05 mm/rev is shown in Fig. 12. No cementite peak can be detected on the surfaces of the drilled holes, which indicated that all the cementite plate has dissolved. The intensity of the austenite peak in drilled fine lamellar pearlite is a little higher than that in drilled coarse lamellar pearlite, which is in agreement with the thickness of the WEL on these two surfaces. For the as-quenched martensite of Fe–0.80% C steel, the volume fraction of austenite is as high as 37% on the surface of the drilled hole. It is reported that the mechanical working of martensitic steel decreases the amount of retained austenite due to strain-induced transformation [20]. Therefore, the austenite present on the surface of a drilled hole is unlikely be of the original matrix structure; rather, it is introduced by the phase transformation from

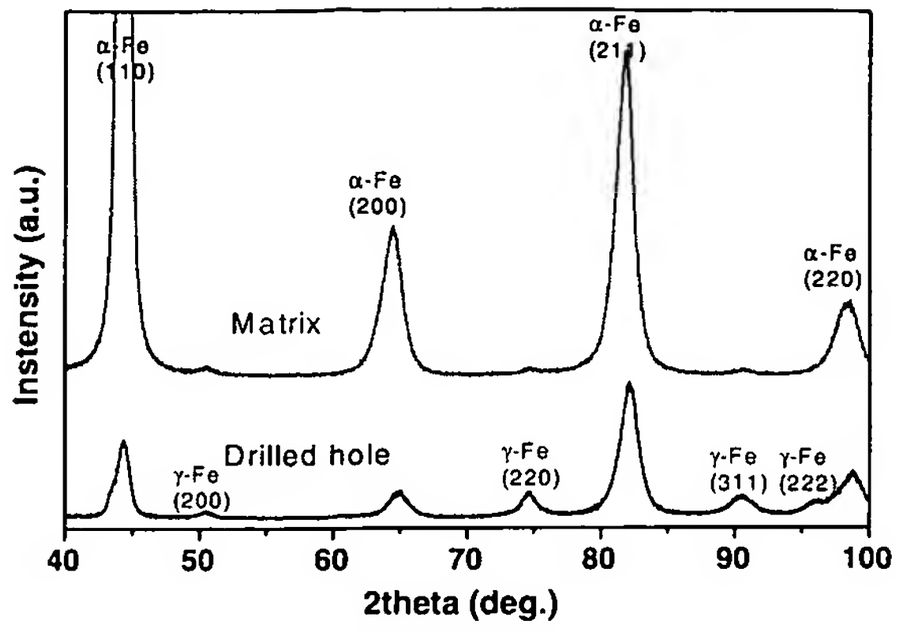


Fig. 12. X-ray diffraction spectra of quenched Fe–0.56% C with different matrix structures after drilling (cutting speed: 80 m/min, feeding rate: 0.05 mm/rev, drill diameter: 5.0 mm).

matrix structure to austenite during drilling. It is noted that the high volume fraction of austenite corresponds well to the thick WEL, which is further confirmation that the WEL is a phase-transformed layer. Compared with the XRD spectrum of the matrix material, it is seen that the ferrite peaks in the XRD spectra of the drilled hole surfaces were broadened (Fig. 11). The broadening of the peak suggests the refinement of grains and an increase in microstrain.

### 3.3. Microhardness near the surface of drilled hole

The hardness distribution profile survey near the surface of drilled holes was carried out along the depth from the surface by a Vickers microhardness tester in SUJ2 steels drilled at different cutting speeds with a feed rate of 0.05 m/min and a drill diameter of 2.5 mm. The results are shown in Fig. 13. It is found that the microhardness value changes with cutting speed and the depth from the hole surface. At a cutting speed of 20 m/min, the surface hardness is lower than that of the matrix, although a deformed structure is observed. The decrease of the surface hardness results from the further tempering of the matrix martensite structure due to the deformation heating. For the surface drilled at a cutting speed of 40 m/min, the decrease of the hardness becomes more severe than that observed at lower cutting speeds. It should be mentioned that the hardness of the WEL on the hole surface drilled at a cutting speed of 40 m/min could not be measured since the layer is too thin to make the measurements. For the surface drilled at a cutting speed of 80 m/min, a hardness of about 9.7 GPa is obtained near the topmost surface. This gradually decreases to 9.2 GPa near the bottom of the WEL due to the increase in grain size. Just below the WEL, the hardness reduces rapidly, reaching a minimum value of approximately 5.8 Gpa, which corresponds to the dark layer, and then increasing gradually back to the matrix hardness of about 7.8 GPa. The characteristics of hardness depth profile for the hole

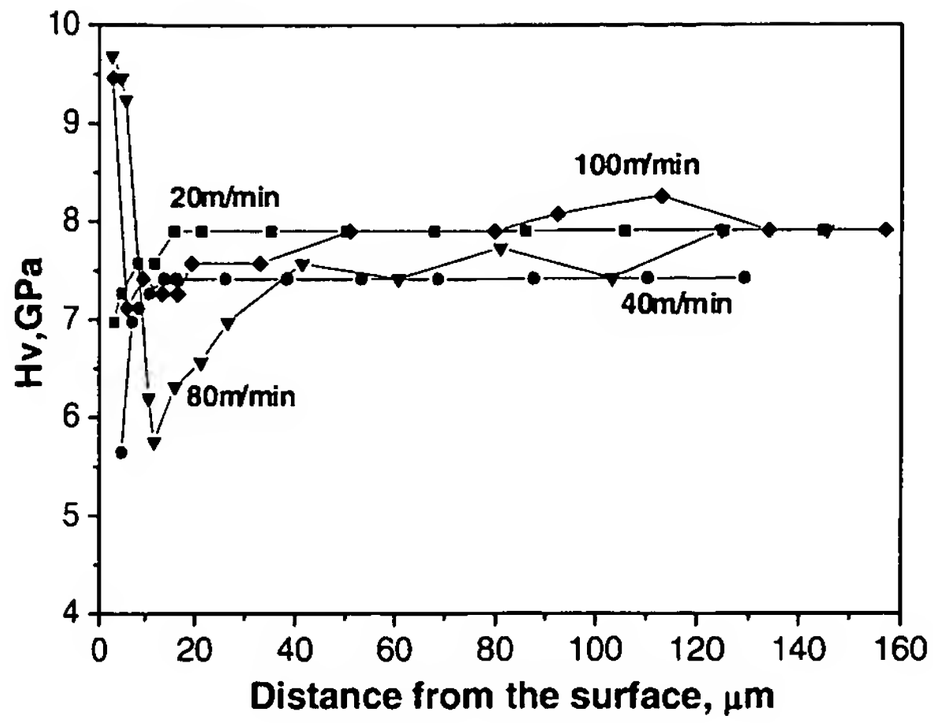


Fig. 13. Microhardness distribution profile near the surface of the drilled hole in SUJ2 steels drilled at different cutting speeds with a feed rate of 0.05 m/min and drill diameter of 2.5 mm.

surface drilled at a cutting speed of 100 m/min is similar to that drilled at 80 m/min, in which the WEL is much harder than the matrix material and the dark layer is softer than the bulk material. It is of interest to note that the hardness of the dark layer produced at a cutting speed of 100 m/min is much harder than that produced at 80 m/min and slightly softer than the matrix. This is considered to improve the performance of the products with drilled holes.

Fig. 14 shows the hardness distribution profile near the hole surface in Fe–0.80% C steels with different matrix structures drilled at a cutting speed of 80 m/min with feed rate of 0.05 mm/rev. For the drilled lamellar pearlite, the hardness monotonously decreases to the matrix hardness with depth from the hole surface. However, for the hole surface of the drilled as-quenched martensite, the WEL is harder than the matrix and the dark layer is softer than the matrix.

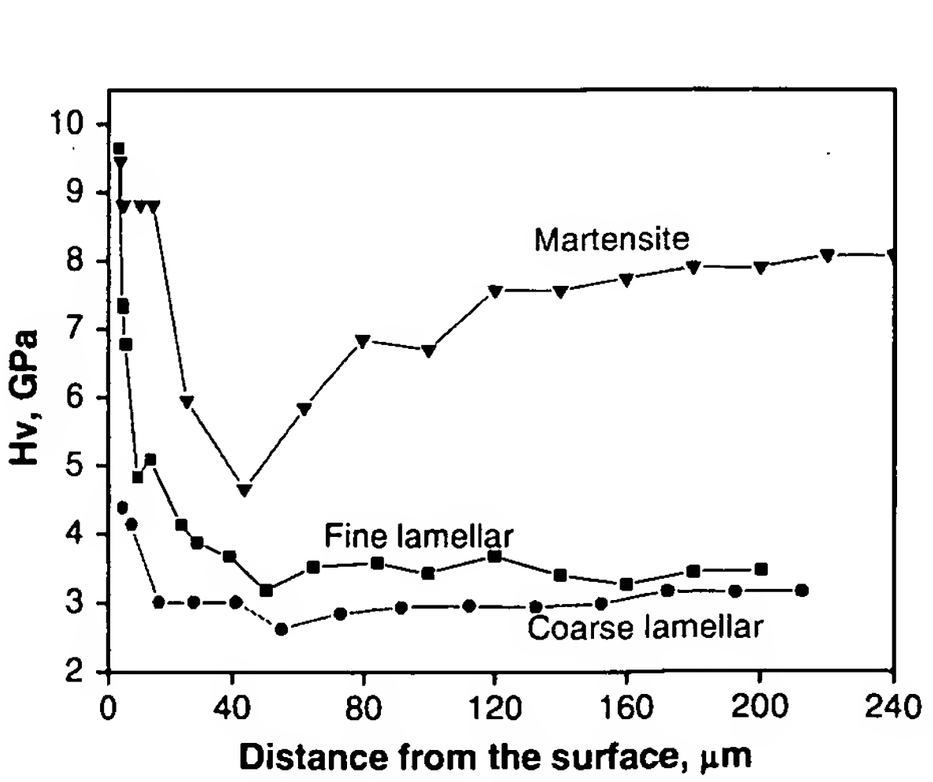


Fig. 14. Microhardness distribution profile near the hole surface in Fe–0.56% C steels with different matrix structures drilled at a cutting speed of 80 m/min with a feed rate of 0.05 mm/rev and a drill diameter of 5.0 mm.

## 4. Discussion

In the present study, the influences of the drilling parameters and matrix structure on drilled holes in various carbon steels have been investigated. The present experimental results provide a description of the process conditions leading to the formation of WELs by drilling and a characterization of the structure and hardness of those WELs. Microstructural observations show that the WELs can be generated on hole surfaces drilled at moderate to high cutting speeds in carbon steels when the matrix hardness is above a certain value, such as with tempered martensite, lamellar pearlite and as-quenched martensite microstructure. This indicates that both drilling parameters and matrix hardness play vital roles in WEL formation. XRD analysis has detected that the amount of austenite presented in the WEL depends on the work materials. The retained austenite content in the WEL formed in Fe–0.80% C carbon steels with an as-quenched martensite structure is as high as 37% in volume fraction, which is significantly higher than that of the matrix. The larger volume fraction of the austenite in WEL than that of its matrix has been reported in the WEL generated by hard turning by, amongst others, Chou and Evans [6], Tönshoff et al. [12], Liermann [21] and Matsumoto [22]. They proposed that the WELs formed on the hard turned surface are a phase-transformed layer. The present study clearly demonstrate that the WEL appearing on the drilled hole surface is also a phase-transformed layer in which re-austenitization has occurred during drilling. Since the phase transformation in the WEL is induced by deformation, we define this kind of phase transformation as dynamic phase transformation (DPT) in order to distinguish it from that which results from pure heat treatment without deformation.

SEM and TEM observations have shown that irregular-shaped submicron grains with a high density of dislocations are generated on the topmost surface of the drilled hole where no WEL has been seen. Equiaxed nanocrystalline structure layers are observed only on the topmost surface of the WEL where DPT occurred. Recently, a number of studies have reported that phase transformation occurred during the formation of the nanocrystalline structure by SPD: for instance, on the surface of hard turned steel [14], ball milled austenitic stainless steel particles [26] and high-pressure torsion-processed high carbon steels [27,28]. Since these phase transformations are induced by deformation, it is quite possible that the phase transformation that occurred in these studies was DPT. Therefore, DPT is considered to play a significant role in the formation of nanocrystalline structure. In practice, DPT has been well known as an effective mechanism to produce ultrafine ferrite grains in steels through the nucleation of new phases at the grain boundary and intragraunlar nucleation during thermomechanical processes [13–15]. However, the DPT in conventional hot and warm rolling processes can only produce ferrite with a grain size of around 1–3 μm [23,24]. It has been reported that the grain size of the final structure

produced by DPT decreases with the increase of strain, strain rate and initial grain size [24,25]. Compared with the traditional thermomechanical processes, one main characteristic of those SPD methods employed to produce a nanocrystalline structure is that a large strain and strain rate can be introduced. Thus the finer grain structure was obtained through DPT induced by SPD. On the other hand, the inhomogeneous deformation with a large strain gradient is another important common characteristic of the aforementioned SPDs used to produce a nanocrystalline structure. Theoretically, a geometrically necessary dislocation (GND) is developed to ensure compatibility of deformation and accommodate strain gradients during inhomogeneous deformation [29,30]. The density of the GND is directly proportional to the strain gradient. The estimations of strain and strain gradient based on the microstructure of the hole surface show that the large strain and strain gradient can be introduced by the drilling process, and they decrease with depth from the top surface [31]. The large strain gradient on the drilled hole surface is beneficial in that it introduces a high density of dislocations, which can evolve into cell or grain boundaries under the large strain deformation, thereby refining the structure. Moreover, the high density of grain boundaries and dislocations provide a very large number of nucleation sites during DPT, which may be expected to lead to further refinement of the microstructure. As a result, the nano- to submicron structure is produced on the hole surface by SPD-induced DPT together with a large strain gradient and high strain rate.

To explain the DPT process induced by SPD in carbon steels, two main mechanisms have been proposed. One is the thermally driven phase transformation mechanism in which the temperature rise is higher than the equilibrium austenite temperature due to the adiabatic deformation heating [14,33,34]. The other is the deformation-driven transformation in which the driving force of DPT is provided by the Gibbs free energy of ultrafine bcc grains together with very high shear stresses far from the conditions predicted according to the equilibrium diagrams [28,32]. In nature, these two mechanisms are very difficult to separate since the SPD is always accompanied by the temperature rise due to deformation heating and the driving forces for the phase transformation and the kinetics of the process can be changed by the superimposed plasticity [35]. Therefore, it is most likely that the two mechanisms act in combination to a lesser or greater degree to produce the DPT. As for which is dominant, it depends both on the alloys and on the deformation conditions [35]. In the present work, although the experiments were performed at room temperature and a coolant was used, the temperature rise produced occurred near the hole surface during high-speed drilling, judging by the surface microstructure observation. The thickness of the nanocrystalline structure layer and the WEL increases with increasing of feed rate, cutting speed and diameter of drill. It is known that increasing the feeding rate, cutting speed, drill diameter and matrix hardness results in an increase in the deformation energy imposed on the surface of the hole, which leads to the increase in temperature. Moreover, the temperature rise causes thermal softening of the material, which contributes to further deformation of the surface layers, causing fragmentation of the grains and an increase of the surface Gibbs free energy. In addition, increasing the matrix hardness by heat treatment with the same chemical composition induces a decrease in thermal stability, which might decrease the phase transformation temperature. According to the above analysis, it is considered that the DPT occurring at the drilled hole surface is introduced by the combination of thermally and deformation-driven structure changes.

The microhardness measurements show that a hardness gradient exists with depth from the drilled hole surface and the hardness depth profile changes with cutting speed and matrix structure. The WEL is formed near the top surface during drilling at moderate to high cutting speed in carbon steels when the matrix hardness is above a certain value. The maximum hardness value of WEL obtained in the present study is about 9.7 GPa, which is much harder than that of as-quenched martensite produced by conventional heat treatment. WELs with extremely high hardness have been reported in many papers on the surface of hard turning [14], wearing [36], grooving [37–39] and shear band [33,34]. In general, the microhardness closely relates to the corresponding microstructure. Louat [40] has proposed that a material consisting of a harder phase and a softer phase, with each phase having a nanocrystalline structure, might have the optimum hardness and strength. In the present study, the microstructural characterization confirms that the topmost surface of the WEL is composed of a mixed structure of equiaxed nanocrystalline ferrite and austenite. Thus, the substantial hardness achieved at the WEL formed on the drilled hole surface was due to the mixture of nanocrystalline soft and hard phases. It is believed that the reported high hardness of WELs [14,33,34,36–39] is also due to the extremely fine grain structures of the ferrite and austenite. During drilling of carbon steels with as-quenched structure, a dark layer is produced beneath the WEL due to the over-tempering of martensite by deformation heating. The dark layer is softer than the matrix, indicating that the effect of softening by tempering is stronger than that of hardening by deformation. In the case of pearlite matrix, a strain-hardened structure layer is generated beneath the WEL during high-speed drilling. Therefore, the hardness continuously decreases with depth from the hole surface.

## 5. Conclusions

In the present study, the microstructure of the drilled hole surface generated under different drilling conditions in carbon steels was investigated by SEM, TEM, XRD and microhardness tester. Based on the present investigation, the following conclusion can be drawn:

1. The surface microstructure depends strongly on the drilling parameters and matrix hardness. When the matrix hardness or cutting speed is low, a deformed structure with a high density of dislocations forms on the topmost surface of the drilled hole. However, WELs can be generated on hole surfaces during drilling at moderate to high cutting speed in carbon steels when the matrix hardness is above a certain value. The WELs are composed of two layers: an equiaxed nanocrystalline structure layer (an average grain size of the order of several tens of nanometers) as an upper layer and a submicron grain layer containing fresh martensite as a lower layer.
2. WEL formation depends strongly on the drilling parameters and matrix hardness. The thickness of the nanocrystalline structure layer and the WEL increase with enhancement of the feed rate, cutting speed, drill diameter and matrix hardness.
3. Microstructural observation and XRD analysis show that the WEL formed on the surface of a drilled hole is a DPT layer. The amount of austenite presented in the WEL depends on the microstructure and alloy compositions of the processed materials.
4. The hardness depth profile near the hole surface changes with the cutting speed and matrix hardness. For the as-quenched martensite matrix, the WEL is much harder and the dark layer is softer than the matrix. In the case of a pearlite matrix, the hardness continuously decreases with depth from the hole surface.
5. It is proposed that the ultrafine structure layer on the surface of the drilled hole is produced by SPD-induced DPT together with a large strain gradient and high strain rate. The DPT that occurs on the drilled hole surface is introduced by both thermally- and deformation-driven phase transformations.

## References


[1] Subramanian K, Cook NH. ASME J Eng Ind 1997;99:295.
[2] Choi Youngsik, Liu CR. Wear 2006;261:485.
[3] Poulachon Gérard, Bandyopadhyay BP, Jawahir IS, Pheulpin Sébastien, Seguin Emmanuel. Int J Mach Tools Manuf 2003;43:139.
[4] Field M, Kahles JF. Ann CIRP 1971;20:153.
[5] Griffiths BJ. J Tribol 1985;107:165.
[6] Chou YK, Evans CJ. Int J Mach Tools Manuf 1999;39:1863.
[7] Barry J, Byrne G. Mater Sci Eng A 2002;325:356.
[8] Shaw MC, Vyas A. Ann CIRP 1994;43:279.
[9] Torrance AA. Wear 1978;50:169.
[10] Kruth P, Stevens L, Froyen L, Lauwers B. Ann CIRP 1995;44: z169.
[11] Field M, Kahles JF. Defense Metals Information Centre Report DMIC; 1964. p. 210.
[12] Tönshoff HK, Brandt D, Wobker H-G, SME Technical Paper MR 95-215; 1995.
[13] Akcan S, Shah S, Moylan SP, Chhabra PN, Chandraseksar S, Yang HTY. Metall Mater Trans A 2002;33A:1245.
[14] Ramesh A, Melkote SN, Allard LF, Riester L, Watkins TR. Mater Sci Eng A 2005;390:88.
[15] Turley DM. Mater Sci Eng 1975;19:79.
[16] Griffiths BJ. J Tribol 1987;109:525.
[17] Inman IA, Datta S, Du HL, Burnell-Gray JS, Luo Q. Wear 2003;254:461.
[18] Tomlinson WJ, Blunt LA, Spraggett S. Wear 1988;128:83.
[19] Guo YB, Schwach DW. Int J Fatigue 2005;27:1051.
[20] Krauss G. Heat treatment and processing principles. Materials Park, OH: ASM International; 1990.
[21] Liermann J, Dr.-Ing. Thesis, WZL-RWTH Aachen, Shaker Verlag; 1988.
[22] Matsumoto Y, Liu CR, Barash MM. High Speed Mach 1984:193.
[23] Hurley PJ, Hodgson PD. Mater Sci Eng A 2001;302:206.
[24] Beladi H, Kelly GL, Shokouhi A, Hodgson PD. Mater Sci Eng A 2004;367:152.
[25] Beladi H, Kelly GL, Shokouhi A, Hodgson PD. Mater Sci Eng A 2004;371:343.
[26] Fujiwara H, Inomoto H, Sanada R, Ameyama K. Scripta Mater 2001;44:2039.
[27] Shabashov VA, Korshunov LG, Mukoseev AG, Sagaradze VV, Makarov AV, Pilyugin VP, Novikov SI, Vildanova NF. Mater Sci Eng A 2003;346:196.
[28] Ivanisenko Y, Maclaren L, Valiev RZ, Fecht H-J. Acta Mater 2006;54:1659.
[29] Ashby MF. Philos Mag 1970;21:399.
[30] Hughes DA, Hansen N, Bammann DJ. Script Mater 2003;48:147.
[31] Li JG, Umemoto M, Todaka Y, Tsuchiya K. J Alloys Compd 2006. doi:10.1016/j.jallcom.2006.08.167.
[32] Ivanisenko Y, Maclaren L, Valiev RZ, Fecht H-J. Adv Eng Mater 2005;7:1011.
[33] Syn CK, Lesuer DR, Sherby OD. Mater Sci Technol 2005;21:317.
[34] Lesuer DR, Syn CK, Sherby OD. Mater Sci Eng A 2005;410-411:222.
[35] Embury JD, Deschamps A, Brechet Y. Scripta Mater 2003;49: 927.
[36] Le Bouar Y, Chaffron L, Saint-Ayes G, Martin G. Scripta Mater 2003;49:985.
[37] Vingsbo O, Hogmark S. Wear 1984;100:489.
[38] Bryggman U, Hogmark S, Vingsbo O. Wear 1986;112:145.
[39] Bryggman U, Hogmark S, Vingsbo O. Wear 1987;115:203.
[40] Louat N. Acta Metall 1985;33:59.